Fuel 281 (2020) 118794

Contents lists available at ScienceDirect

Fuel

journal homepage: www.elsevier.com/locate/fuel

Full Length Article

Dilution gas and hydrogen enrichment on the laminar flame speed and flame structure of the methane/air mixture

Xiongbo Duan[a], Yangyang Li[a,*], Yiqun Liu[b], Shiheng Zhang[a], Jinhuan Guan[a], Ming-Chia Lai[b], Jingping Liu[a]

[a] State Key Laboratory of Advanced Design and Manufacturing for Vehicle Body, Hunan University, Changsha 410082, China
[b] Department of Mechanical Engineering, Wayne State University, 5050 Anthony Wayne Dr., Detroit, MI 48202, USA

ARTICLE INFO

Keywords:
Dilution gas
Hydrogen enrichment
Laminar flame speed
Flame structure
Flame instability

ABSTRACT

In this study, the mechanisms of the chemical, thermal and dilution effects of the CO_2, H_2O, N_2 and EGR quantitatively analyzed on the laminar flame speed, laminar flame structure and key radicals profiles of the premixed methane/air mixture. Moreover, the artificial species of the FCO_2, FH_2O, FN_2 and FEGR were used to separate the combined chemical and physical effects. Furthermore, the impacts of the hydrogen enrichment coupled with the EGR on the laminar flame speed, the laminar flame structure and key radicals profiles of the premixed methane/air mixture was also studied in detailed. The results indicated that the chemical effect of the CO_2 dilution gas produced the greatest impacts on the laminar flame speed, adiabatic combustion temperature and key radicals formation of the methane/air, and followed by the H_2O vapor, EGR and N_2. In addition, the dilution limitation of the CO_2 in the methane/air was smallest, followed by the H_2O vapor, EGR and N_2. Moreover, the thermal effect of the CO_2 in the methane/air was strongest due to its highest specific heat capacity, followed by the H_2O vapor, EGR and N_2. The laminar flame speed and adiabatic combustion temperature of the methane/hydrogen/air increased with increasing the hydrogen. Furthermore, the lean-burn limitation of the methane/air was extended with the increase of the hydrogen. The radical pool, such as H, O, OH, accelerated the chain branching reactions and the chain propagation reactions, and thereby increasing the effect of the chemical amplifier during the combustion of the premixed methane/air mixture.

1. Introduction

In order to reduce the toxic emissions and green gas in the real combustion applications, such gas turbine, internal combustion engine, power plants, and burner, it is paramount to achieve clean combustion and higher efficient [1,2]. Currently, the modern advanced applications are widely introduced some additives or diluents (reactive species [3,4], diluted gas [5] and their combinations [6,7]) in the combustion system or the flame to control the pollutant emissions formation, stabilize the flame, accelerate or suppress of identified chemical reactions [8-11]. Technically, the diluted gases exert profound influences on the combustion processes through the three following factors: (a) the dilution effect was attributed to partially substitute the reactants in the reactive mixture and ultimately decrease the reactants concentration; (b) the thermal effect was caused by partial absorption the heat released energy from the chemical reactions due to higher specific heat capacity, and thereby resulting in a reduction in the adiabatic flame temperature; (c) the chemical effect was owing to the activity of the diluted gas that may react with some radicals and compete with some reactions, and thereby changing some the directions of different chemical reactions [12]. Furthermore, these three factors are concomitant and closely linked with each other.

On the one other hand, the laminar flame speed is generally defined as the velocity at which the flame of the fresh premixed combustible gas achieves a steady-state relative to the unburned gas [13]. Furthermore, the flame is assumed to be planar, unstretched, and adiabatic, which meant the flame reaches chemical equilibrium between the burned gas and the unburned gas. In addition, the laminar flame speed is heavily affected by the specific composition of the mixture, the initial temperature and the initial pressure. On the other hand, from the respect of the practical application, the laminar premixed flame is widely used in daily life, including the flat-burner. Plus, studying the laminar burning velocity and flame structure of the premixed combustible gas [14] aim at to obtain an in-depth understanding the combustion properties and chemical reaction kinetics characteristics of different type fuels [15], which are conducive to optimizing the combustion process, increasing

* Corresponding author.
E-mail address: 982807258@qq.com (Y. Li).

https://doi.org/10.1016/j.fuel.2020.118794
Received 11 May 2020; Received in revised form 1 July 2020; Accepted 21 July 2020

the combustion efficiency and reducing toxic emissions. In addition, from the point of a more fundamental research, the laminar flame speed is widely used to verify and revise various developed chemical reaction mechanism of different hydrocarbon fuels (including a detailed chemical reaction mechanism, the skeleton chemical reaction mechanism and the simplified chemical reaction mechanism), modify or optimize the specific the coefficient of reactions [16], and also supply the basic data for simulating the turbulent premixed combustion flame propagation [17]. Laminar flame speed is also a key parameter to describe various combustion phenomena (flame stabilization, flame flashback and flame blowing and flame extinguishing). Consequently, studying the laminar flame speed and flame structure by combining experiments and numerical simulation can get an insight into the combustion process, and understand the turbulent combustion process, and provide fundamental data for developing surrogate fuel models and validating the turbulence models [18]. Subsequently, all kinds of experimental methodologies have been developed to measure the laminar flame speed by using various flame configurations, for instance, the Bunsen flame [19], flat-burner flame [20], counterflow/stagnation flame [21], and spherical flame [22]. Egolfopoulos et al. [23] currently reviewed the merits and demerits of these mentioned flame configurations in detailed.

In addition, it is widely accepted that introducing the exhaust gas recirculation (EGR) in the combustible gas results in remarkably changing the fundamental flame properties, including the laminar flame speed, adiabatic flame temperature and flame structure [24,25], and thereby affecting the pollution emissions formation, such as nitrogen oxide (NOx), carbon monoxide (CO), unburned hydrocarbon (HC), and particle matter (PM). Generally, the compositions of the EGR imported from the traditional hydrocarbon fuels operating at stoichiometric air–fuel ratio conditions are mainly nitrogen (N_2), carbon dioxide (CO_2), water vapor (H_2O) and other pollution emissions NOx, CO, and HC [26]. Admittedly, the main compositions of the N_2, CO_2, and H_2O in the EGR will definitely affect the laminar flame speed and the flame structure of the fuel. Therefore, it is paramount to investigate the absolute influences of individual or combined dilution gases on the combustion characteristics of premixed methane/air mixture different initial temperatures and pressures. Many researchers conducted experiments and simulations on the premixed laminar methane/air flames to investigate the fundamental influences of each N_2, CO_2, and H_2O dilution gases [7,27,28]. Fells et al. [29] employed the conical flame method to measure the laminar flame speed of the methane-air mixture with or without N_2 and CO_2 dilution gases at atmospheric conditions. They reported that the effect of the CO_2 in the methane-air mixture on the laminar flame speed was obviously higher than that of the N_2. Kan et al. [30] study the dilution effects of the N_2 and CO_2 on the laminar flame speed of the premixed methane-air mixture by using the freely expanding spherical flames. They concluded that the laminar flame speed of the mixture was considerably decreased with addition of diluents due to the reduction in energy content of the reactants, increase in the specific heat capacity of the mixture and the corresponding decrease in the adiabatic flame temperature during the combustion process. In addition, they also found that the Markstein length of the burned gas remained positive, which indicated that the mixture was stable towards the differential diffusion effects. Mazas et al. [12] adopted the axisymmetric burner to investigate the influences of the steam dilution (H_2O vapor) with O_2 enriched in the methane flames at atmospheric pressure. They showed that the laminar flame speed of the methane-air mixture was decreased quasi-linear with increasing H_2O vapor molar fraction. Albin et al. [31] investigated the influence of H_2O vapor dilution on the laminar and turbulent methane-air flames at atmospheric pressure by using the Bunsen and lifted turbulent V-flames. The results indicated that the methane–air flame in high H_2O vapor dilution condition was three times slower than that without H_2O vapor dilution condition. Xie et al. [32] reported that CO_2 showed a stronger chemical effect than H_2O. In addition, the intrinsic flame instability was promoted at atmospheric pressure and was suppressed at elevated pressure for the CO_2 and H_2O diluted mixtures. Apparently, with adding the N_2, CO_2, and H_2O dilution gas in the methane-air mixture, the laminar flame speed is decrease due to the chemical and physical effects. Consequently, some researchers added the reactive specie (such as hydrogen) in the diluted methane-air mixture to improve the combustibility of the hydrocarbon fuels and balance the toxic emission formation because it could significantly decrease the ignition energy, improve the burning speed and the adiabatic combustion temperature [33]. Schefer et al. [34] conducted experiments on the premixed, swirl-stabilized flame to investigate the combustion characteristics of the hydrogen-enriched methane-air mixture at lean-burn conditions. They observed that the lean blow-off stability limit was extended with adding the hydrogen in the methane-air mixture. Moreover, the OH-PLIF data demonstrated that the hydrogen-enriched remarkably increased the concentrations of OH radical during the combustion process, which was a key specie during the hydrocarbon fuels oxidation processes. Ilbas et al. [35] also experimentally investigated the laminar flame speed of the hydrogen–methane mixture and showed that the laminar flame speed was increased with increasing the hydrogen percentage and extended the flammability limitation of the mixture. These investigation showed that the addition of CO_2 directly participated the reaction through $OH + CO = CO_2 + H$ during the combustion process, which of course suppressed the reaction and limited the main exothermic reaction, and thereby decreasing the adiabatic combustion temperature and the laminar flame speed. However, the addition of H_2 increased the adiabatic combustion temperature and the laminar flame speed, and decreased the laminar flame thickness and Markstein length [36], due to dramatically increase the H, OH, etc. radicals pool during the combustion process.

As evident from the mentioned experimental and simulation investigations, additions of the individual and multiple dilution gases (N_2, CO_2, and H_2O, and even their combinations) to the methane-air mixture resulted in a decreased laminar flame speed, while addition of the reactive specie (hydrogen) led to an increased laminar flame speed. However, the detailed mechanisms of the chemical, thermal and dilution effects of the additions on the laminar flame speed of the methane-air mixture could not completely separately during the experiments. Furthermore, most of the experiments data reported in the literature investigated the global effects of the diluents with N_2, CO_2, H_2O, and even their combinations (mimic EGR) on the laminar flame speed of the methane-air-diluent mixture. Consequently, it is a challenge in understanding the each effects of the diluents on the laminar flame speed of the methane-air in the experiment, not to mention coupling with the hydrogen for extending the lean-burn limitation. This study therefore aimed at to study their respective influence of the CO_2, H_2O, N_2 and their combination and hydrogen on the laminar flame speed of the methane/air mixture. First, the laminar flame speed of the methane/air mixture with CO_2, H_2O, N_2 and their combination and hydrogen were calculated and compared with the experiment data in the literature. Then, in order to quantitatively evaluate the mechanism of the chemical, thermal and dilution effects, the fictitious species of the FCO_2, FH_2O, FN_2 and FEGR were employed in this simulation study, while maintained the same thermal and transport properties, but not participated any reactions during the combustion. Last, the effects of the hydrogen coupled with EGR were also comprehensively investigated on the laminar flame speed and flame structure of the methane/air mixture.

2. Theoretical analysis and computational methods

Generally, the thickness of the laminar premixed flame is extremely thin during the combustion process. The thin-layer of the laminar premixed flame separates the burned zone and the unburned zone, which shows a high temperature gradient and concentration gradient between the burned zone and the unburned zone, and thereby driving

the heat and mass transfer fiercely at the flame front. In addition, once the combustion process is initiated, the laminar premixed flame will sustains itself by burning fresh combustible mixture [37]. Furthermore, the layer of the laminar premixed flame could continue to divide into the preheat zone and reaction zone during the combustion process. Interestingly, the preheat zone takes up a large part of the layer of the laminar premixed flame, in which the mixture is continuously heated, the heat and initial radicals are mainly diffused from the reaction zone to the preheat zone, and the chemical reaction rate is very low. The reaction zone is also continually divided into the fast-reaction zone and slow-reaction zone‘. In the fast reaction zone, the combustible mixture is consumed and generated a large number of intermediate components and radicals, in which the main reaction is the bimolecular reaction. While the slow-reaction zone is dominated by three free radical synthesis reactions, so the reaction rate is much slower than that of a typical bimolecular reaction. In addition, the upstream and downstream flow velocity of the laminar premixed flame are accelerated due to the increase of the density. The flame radiation is mainly located in the fast-reaction zone, and the color of the laminar premixed flame is heavily determined by the equivalent ratio of the mixture and the combustion temperature [38].

In this study, in order to obtain the laminar flame speed, the flame structure and radical profiles of the methane/air mixture with dilution gases and hydrogen, the detailed methane/air combustion mechanism, GRI-Mech. 3.0 [39], was used in this work. Furthermore, the unstretched, adiabatic and freely-propagating planar flame was employed in this paper by using the Chemkin code to solve the steady-state mass, species, energy conservation equations [40]. The number of grid points was maintained at 1000 so that the simulated laminar flame speed and the flame structure of the methane/air were grid-independent. In addition, the adaptive grid was employed during the simulation [41]. The initial temperature was set at 393 K according to the experiment data in ref. [42]. The computational domain of the laminar flame of the methane/air was fixed from −0.2 to 1 cm. The convection term in the simulation was discretized by adopting the windward difference method. The average method was used to calculate the diffusion coefficient of the mixture during the simulation. In addition, the Soret effect was also taken into account during the simulation [28]. Last, the relative and absolute errors in the iterative process during the simulation less than 10^{-6}, which was fully satisfied the calculation requirements during the simulation.

When the methane/air mixture is completely burned at the stoichiometric air–fuel ratio as expressed in equation (1), the residual gas and combustion products are the N_2, H_2O and CO_2, and their percentages are 71.59%, 18.94% and 9.47%, respectively. In order to simulate the effects of the EGR on the laminar flame speed and the flame structure on the methane/air mixture, the mentioned percentage of the N_2, CO_2 and H_2O in the EGR were directly inputted as the boundary conditions.

$$CH_4 + 2(O_2 + 3.76N_2) = CO_2 + 2H_2O + 7.52N_2 \quad (1)$$

Therefore, the chemical reaction equation of the methane/air mixture with dilution gases at the stoichiometric air–fuel ratio could be written as equation (2), while the dilution ratio was defined as equation (3). In addition, the hydrogen ratio in the oxidizer was expressed as equation (4) as following.

$$CH_4 + 2(O_2 + 3.76N_2) + \alpha Diluent = CO_2 + 2H_2O + 7.52N_2 + \alpha Dilutent \quad (2)$$

$$\phi_{dilution} = \frac{\alpha_{dilution}}{n_{CH_4} + n_{O_2} + n_{N_2} + \alpha_{dilution}} \quad (3)$$

$$R_H = \frac{n_{H_2}}{n_{CH_4} + n_{H_2}} \quad (4)$$

where $\alpha_{dilution}$, n_{CH_4}, n_{O_2}, $n_{N_2}$and $n_{H_2}$are the mole fraction of the diluents, methane, oxygen, nitrogen and hydrogen in the mixture, respectively.

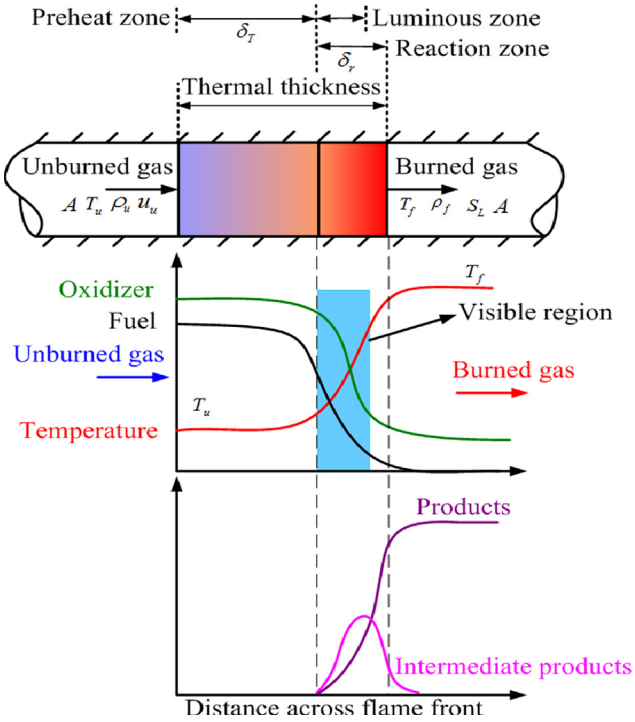

Fig. 1. The flame structure of the 1D laminar flame.

$R_H$is the ratio of the hydrogen in oxidizer. It is noted that the $\alpha_{dilution}$ could be represented the EGR by inputting the specific ratios of the CO_2, H_2O and N_2 in the diluent Fig. 1.

3. Results and discussion

3.1. Effects of dilution gas on the laminar flame speed and the flame structure of the premixed methane/air

Fig. 2 illustrates the effects of various dilution gases on the laminar flame speed of the methane/air at the stoichiometric air–fuel ratio, initial temperature 393 K and initial pressure 1 bar. In order to make sure the water existed as the water vapor in the methane/air, the relative high initial temperature was selected in this paper according to the literature [42]. As shown in the Fig. 2, the laminar flame speed and flame instability of the methane/air were obviously different with adding different dilution gases. As displayed in the Fig. 2 (a), with increasing the percentage of the CO_2, the laminar flame speed of the methane/air significantly decreased, and its change trend was nonlinear. While with increasing the ratio of the FCO_2, namely excluding the chemical effect, the laminar flame speed of the methane/air moderately declined, which was mainly caused by the dilution and thermal effects of the FCO_2. Furthermore, the decreasing magnitude caused by the FCO_2 was relatively weaker on the laminar flame speed of the methane/air compared with the CO_2, and its change trend was almost linear. These were attributed to the following reasons. First, the reactions of the OH + CO = CO_2 + H and CO + O_2 = CO_2 + O were the main chain propagation reactions and primary pathways of the oxidation of CO into CO_2. With increasing the concentration of CO_2, the reactions of the OH + CO = CO_2 + H and CO + O_2 = CO_2 + O were reversed via shifting the chemical equilibrium. In addition, the H radical and O radical also consumed due to the backward reactions, and therefore the combustion rate of the premixed flame of the methane/air mixture was limited, and thereby decreasing the laminar flame speed due to the prime chemical effect. Moreover, the third-body effect of CO_2 also affected combustion of the methane/air and shifted the reaction of the H_2O + M = H + OH + M backward. Most importantly, the

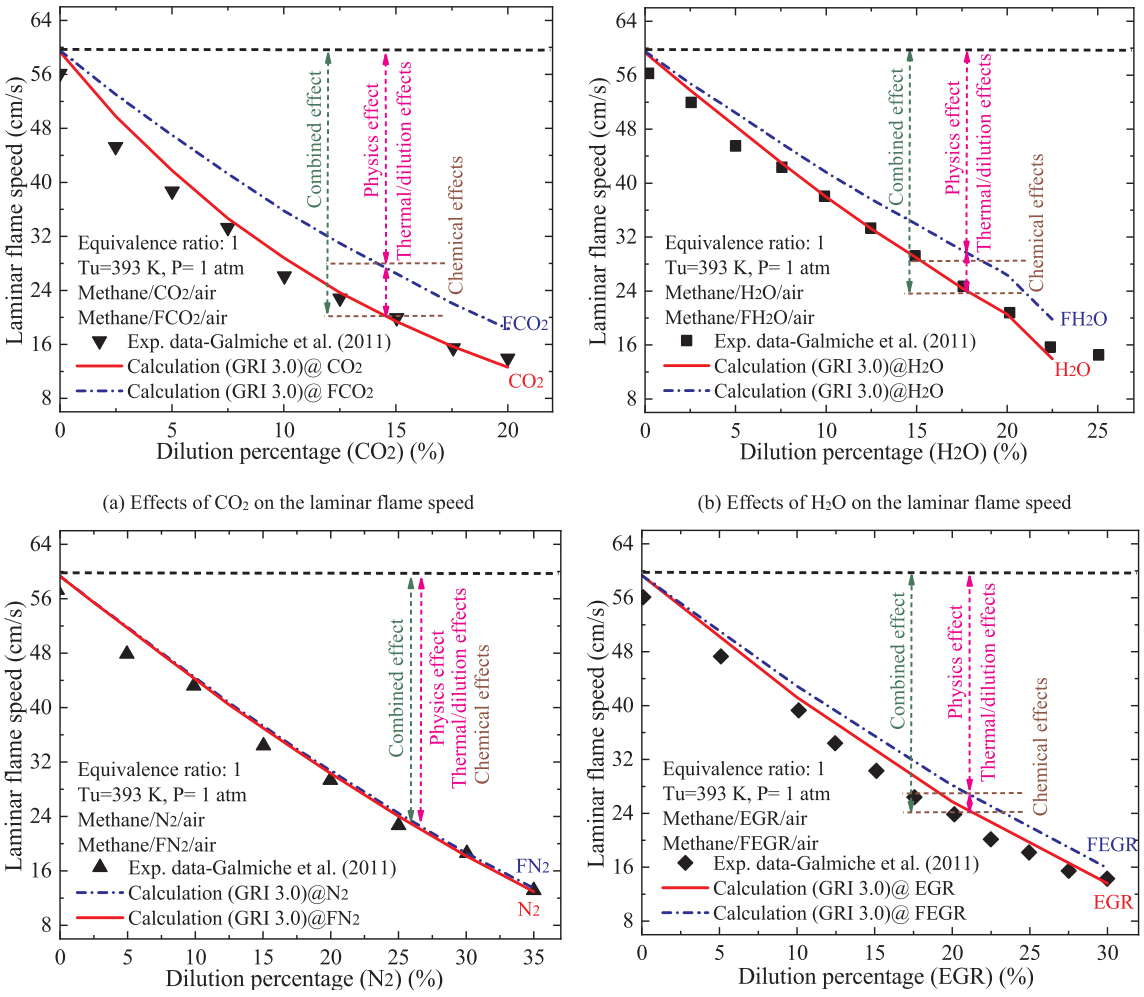

(a) Effects of CO_2 on the laminar flame speed

(b) Effects of H_2O on the laminar flame speed

(c) Effects of N_2 on the laminar flame speed Flame

(d) Effects of EGR on the laminar flame speed Flame

Fig. 2. The effects of diffident dilution gases on the laminar flame speed of the methane/air.

OH + CO = CO_2 + H was the dominating exothermic reaction during the combustion. Thus, the adiabatic combustion temperature of the methane/air mixture descended with increasing the CO_2 ratio. Of course, the O、H、OH、CH_3 radicals would greatly decrease with decreasing the combustion temperature. In addition, the heat and mass transfer rate between the burned gas and unburned gas also decreased during the combustion due to the limited Soret diffusion effect. Last, the reactant concentration of the methane/air definitely decreased with increasing the increasing the concentration of CO_2, which, of course, decreased the effective collision probability of the methane and oxygen molecules, and thereby resulting in decreasing the laminar flame speed of the methane/air. However, with increasing the concentration of FCO_2, the chemical effect could be considered negligibly because the FCO_2 did not participate the reactions of the OH + CO = CO_2 + H and CO + O_2 = CO_2 + O. And the physics effect of the FCO_2, including the thermal and dilution effects, played a decisive role in the reduction of the laminar flame speed of the methane/air. Last, according to ref. [43], the laminar flame speed and the flame instability of the methane/air were determined by the effects of hydrodynamic and thermal-diffusive. As illustrated in the Fig. 2 (b), with increasing the percentage of the H_2O, the laminar flame speed of the methane/air moderately decreased, and its change trend was almost linear, and so did the FH_2O on the laminar flame speed of the methane/air. With adding the H_2O vapor in the methane/air mixture, the reaction of the H_2O + O = OH + OH was favors O radical consumption [12], which inhibited the methane oxidation through the reaction of CH_4 + O = CH_3 + OH. In addition, the reaction of the OH + CH_4 = CH_3 + H_2O was suppressed by the chemical effect of the H_2O vapor. Furthermore, according to Le Cong and Dagaut computations, the H_2O vapor would promote the reaction of the H + O_2 + M = HO_2 + M, particularly at the lower temperature due to its higher chaperon efficiency [44]. And this reactions will competed with the main branching reaction of the H + O_2 = HO + O, and led to convert the high reactive H radical into the less reactive HO_2 radical. However, with increasing the concentration of FH_2O, the chemical effect was insignificant due to without involving the reactions of the H_2O + O = OH + OH and CH_4 + O = CH_3 + OH. And the thermal and dilution effects of the FH_2O was also played a principal role in the reduction of the laminar flame speed of the methane/air. As demonstrated in the Fig. 2 (c), with increasing the percentage of the N_2 or the FN_2, the laminar flame speed of the methane/air greatly decreased, and their change trends were almost the same. Obviously, the chemical effect of the N_2 on the laminar flame speed of the methane/air could completely ignore. Thus, the physics effect of the N_2 took the full responsibility for decreasing the laminar flame speed of the methane/air. As demonstrated in the Fig. 2 (d), with increasing the percentage of the EGR, the laminar flame speed of the methane/air decreased, and its change trend was non-linear due to the effect of the CO_2. In addition, the chemical effect of the EGR on the laminar flame speed was weaker than that of the CO_2 and H_2O due to the fact that the main composition was N_2 (the percentages of the N_2, H_2O and CO_2 are 71.59%, 18.94% and 9.47%). In summary, the physics effect of the dilution gas was stronger than that its chemical effect. In addition, the chemical effect of

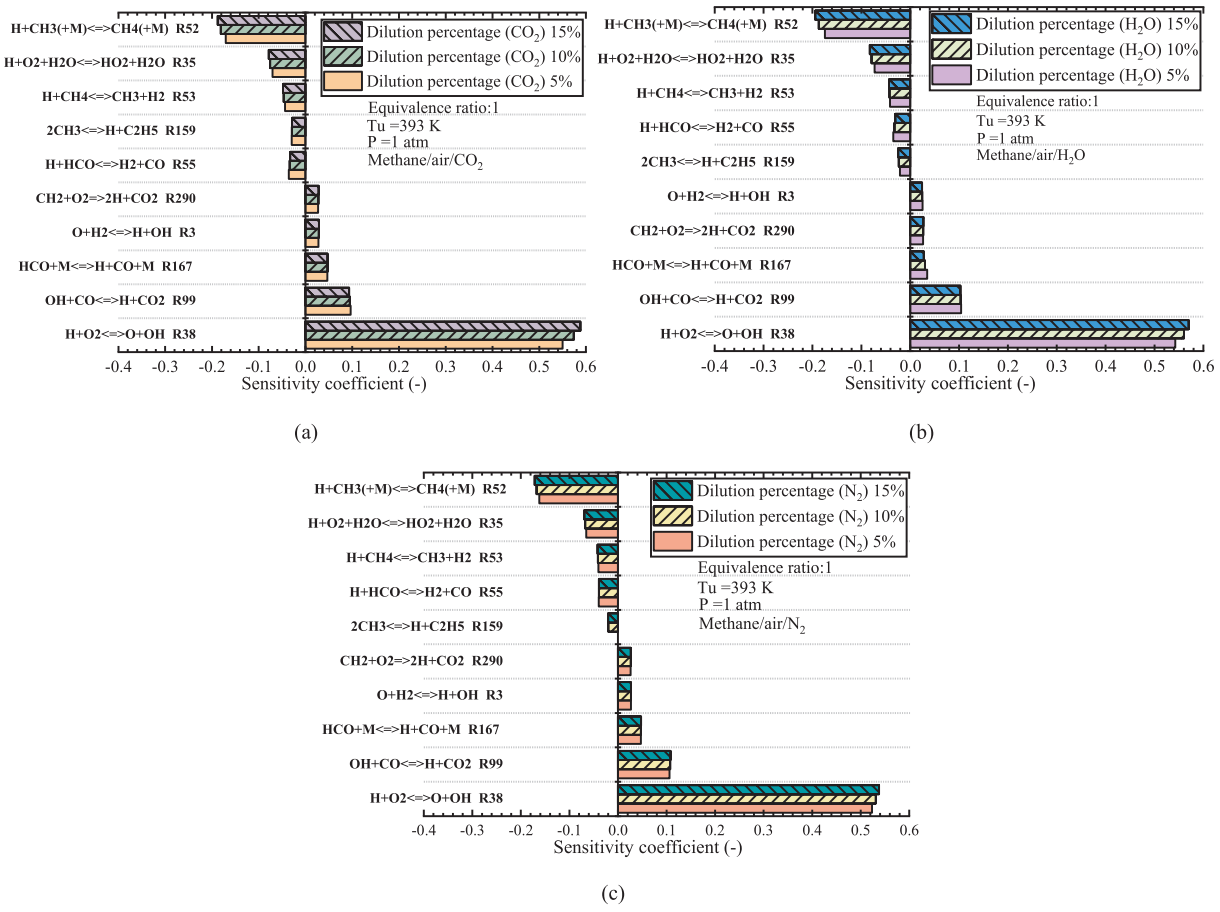

Fig. 3. The effects of different dilution gas contents on sensitivity coefficient of mass burning rates of main elementary reactions.

the CO_2 exerted greatest effect on the laminar flame speed of the methane/air compared to other dilution gases, followed by the H_2O, EGR and N_2. Furthermore, the laminar flame speed and the flame instability of the methane/air were determined by the effects of hydrodynamic and thermal-diffusive.

Fig. 3 depicts the effects of different dilution gas contents (CO_2, N_2 and H_2O) on sensitivity coefficient of mass burning rates of main elementary reactions. Generally, if the sensitivity coefficient of the main elementary reaction is positive, it indicates that this reaction promotes the laminar flame speed; while the sensitivity coefficient of the main elementary reaction is negative, it indicates that this reaction inhibits the laminar the laminar flame speed. Obviously, the main elementary reactions of the $H + O_2 = O + OH$, $O + H_2 = H + OH$ and $OH + CO = H + CO_2$, etc. are beneficial to increase the laminar flame speed. Furthermore, the CO_2 produced the greatest impacts on sensitivity coefficient of mass burning rates of the main elementary reactions (such as $H + O_2 = O + OH$), and followed by the H_2O vapor, EGR and N_2. Moreover, the sensitivity coefficient of elementary reaction of the $H + O_2 = O + OH$ increased with increasing the dilution ratio. In addition, the absolute value of the sensitivity coefficient of elementary reaction of the $H + CH_3 + M = CH_4 + M$ was also increased with the increase of the dilution ratio. Furthermore, the termination reaction of the $H + CH_3 + M = CH_4 + M$ would suppress the laminar flame speed of the methane/air mixture. These radicals were produced or consumed by the chain branching, chain propagation and termination reactions during the combustion, which, of course, ultimately affected the laminar flame speed of the methane/air mixture.

Fig. 4 demonstrates the flame structure and radical reaction rate profiles of the methane/air at the stoichiometric air–fuel ratio, initial temperature 393 K and initial pressure 1 bar without dilution gas addition. As shown in Fig. 4 (a), without adding the dilution gas, the adiabatic combustion temperature of the methane/air was much high and surpassed 2100 K, which was beneficial to increase the thermal diffusion, the molecular diffusion and the number of effective collisions, decrease the activation energy required for the reactions, and thereby generating lots of O, H, OH and CH_3 radicals (as illustrated in Fig. 4 (b)), and accelerating the chain branching reactions of the $O + CH_4 = OH + CH_3$, $H + O_2 = O + OH$, $H + HO_2 = 2OH$, and $O + H_2 = H + OH$, and the chain propagation reactions of the $OH + CH_4 = CH_3 + H_2O$ and $H + CH_4 = CH_3 + H_2$. These radicals were produced by the chain branching and chain propagation reactions during the combustion, and thereby ultimately accelerating the combustion rate. In addition, the CO could not fully convert into the CO_2 through the reactions of the $OH + CO = CO_2 + H$ and $CO + O_2 = CO_2 + O$ due to the effect of the chemical equilibrium, and eventually reach the equilibrium state. Consequently, controlling or inhibiting the reactions of these chain branching and propagation reactions could effectively control the reaction rate and alter the direction of chemical equilibrium, which were conducive to reducing the toxic emissions formation.

Fig. 5 depicts the effects of the CO_2 dilution gas addition on the flame structure and radical reaction rate profiles of the methane/air at the stoichiometric air–fuel ratio, initial temperature 393 K and initial pressure 1 bar. As presented in Fig. 5 (a), the adiabatic combustion temperature of the methane/air was obviously decreased and slightly exceeded 1800 K with 20% CO_2 dilution gas addition. Moreover, the O, H, OH and CH_3 radicals also dramatically decreased with 20% CO_2 dilution gas addition (as shown in Fig. 5 (b)). These phenomena was attributed to the following reasons. First, as stated earlier, the main exothermic reaction of the $OH + CO = CO_2 + H$ was heavily suppressed, and even reversed with increasing the concentration of CO_2 due to its chemical effect, and thereby decreasing the adiabatic

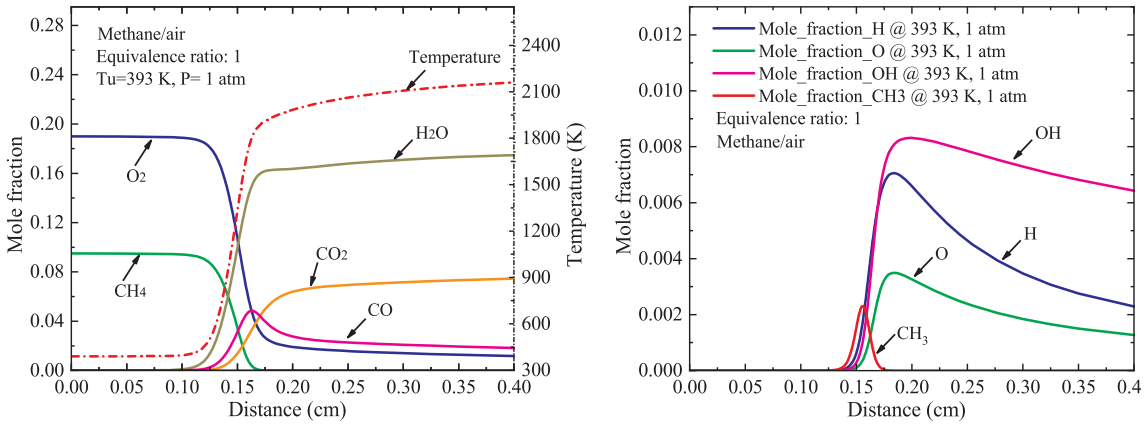

(a) Flame structure profile without dilution gas addition.

(b) Radical reaction rate profiles without dilution gas addition.

Fig. 4. The key radical reaction rate and flame structure profiles of the methane/air at 393 K and 1 atm without dilution gas addition.

combustion temperature. In addition, the concentration of the methane/air was decreased with adding the CO_2 due to its dilution effect, and the thermal properties, transport properties and reaction rate were also decreased, and the heat released during the combustion process was also declined, which could in turn affect the adiabatic combustion temperature and constrain radicals' formation. Most important, the laminar flame of the methane/air was instability, and was very insensitive to the CO_2 dilution gas.

Fig. 6 delineates the impacts of the H_2O dilution gas addition on the flame structure and radical reaction rate profiles of the methane/air at the stoichiometric air–fuel ratio, initial temperature 393 K and initial pressure 1 bar. As shown in Fig. 6 (a), with adding the 20% H_2O dilution gas in the methane/air mixture, the adiabatic combustion temperature of the methane/air was also declined, but slightly higher than that of introducing 20% CO_2 dilution gas (as shown in Fig. 5 (a)). In addition, with importing the 20% H_2O dilution gas in the methane/air mixture, the O, H, OH and CH_3 radicals also moderately decreased, but their mole fractions were higher than that of introducing 20% CO_2 dilution gas (as shown in Fig. 5 (b)), particularly the OH radical. Furthermore, the concentration of the methane/air was also decreased with adding the H_2O due to its dilution effect, which resulted in decreasing the concentrations of different radicals and heat release, and thereby decreasing the adiabatic combustion temperature of the methane/air.

Fig. 7 portrays the influences of the N_2 dilution gas addition on the flame structure and radical reaction rate profiles of the methane/air at the stoichiometric air–fuel ratio, initial temperature 393 K and initial pressure 1 bar. As shown in Fig. 7 (a), with adding the 20% N_2 dilution gas in the methane/air mixture, the adiabatic combustion temperature of the methane/air also descended, but slightly higher than that of introducing 20% CO_2 and 20% H_2O dilution gases. Although the O, H, OH and CH_3 radicals also decreased with importing the 20% N_2 dilution gas in the methane/air mixture, but their mole fractions were higher than that of introducing 20% CO_2 and 20% H_2O dilution gas. In addition, the mole fractions of the O and H radicals were much higher than that of introducing the CO_2 and H_2O dilution gases in the methane/air mixture as illustrated in Fig. 7 (b). The O and H radicals would accelerate the chain branching reactions of the $O + CH_4 = OH + CH_3$, $H + O_2 = O + OH$, $H + HO_2 = 2OH$, and $O + H_2 = H + OH$, and the chain propagation reactions of the $OH + CH_4 = CH_3 + H_2O$ and $H + CH_4 = CH_3 + H_2$. Therefore, the chemical effect of the N_2 dilution gas on the laminar flame speed of the methane/air could be ignored. Furthermore, the N_2 is the diatomic molecule, and the specific heat capacity of the N_2 (29.3 J/(mol·K)) is smaller than that of the triatomic molecules of the CO_2 (41 J/(mol·K)) and H_2O (34.2 J/(mol·K)). Consequently, the thermal effect of the N_2 on the adiabatic combustion temperature and laminar flame speed of the methane/air was weaker than that of the CO_2 and H_2O. That is also why that the dilution limitation of the N_2 in the methane/air mixture was wider than that of the CO_2 and H_2O.

Fig. 8 describes the effects of the EGR on the flame structure and radical reaction rate profiles of the methane/air at the stoichiometric air–fuel ratio, initial temperature 393 K and initial pressure 1 bar. As illustrated in Fig. 8 (a), with adding the 20% EGR in the methane/air

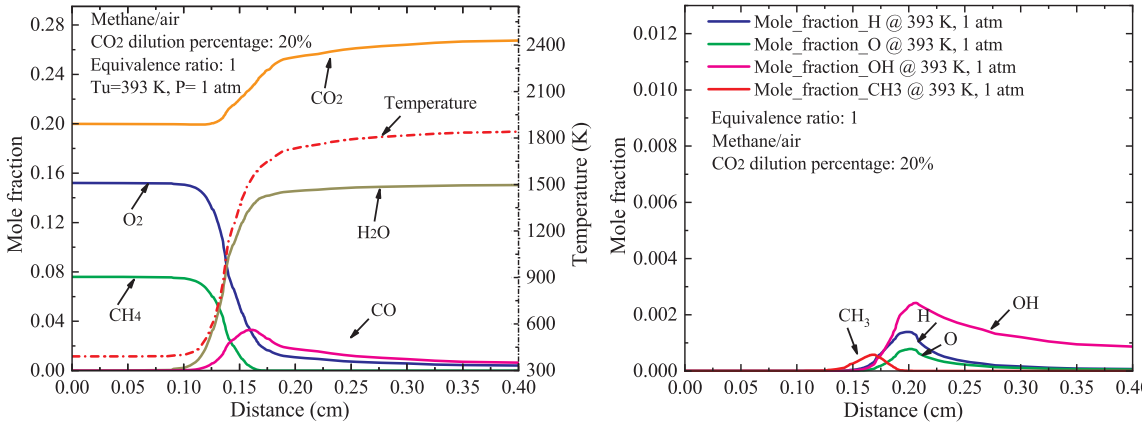

(a) Flame structure profile with CO_2 addition.

(b) Radical reaction rate profiles with CO_2 addition.

Fig. 5. The flame structure and key radical reaction rate profiles of the methane/air at 393 K and 1 atm with CO_2 addition.

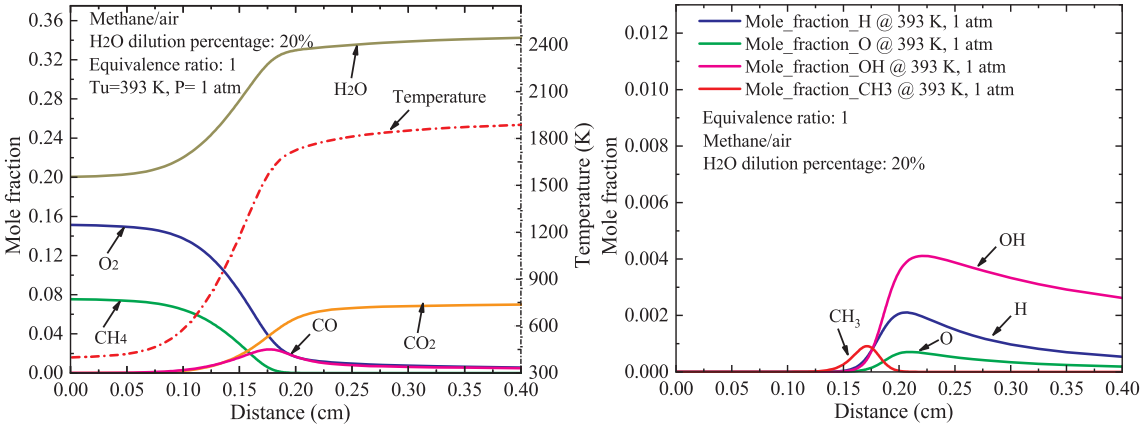

(a) Flame structure profile with H_2O addition. (b) Radical reaction rate profiles with H_2O addition.

Fig. 6. The flame structure and key radical reaction rate profiles of the methane/air at 393 K and 1 atm with H_2O addition.

mixture, the adiabatic combustion temperature of the methane/air also decreased. Since the EGR contained the percentages of the N_2, H_2O and CO_2, and their ratios were 71.59%, 18.94% and 9.47%, respectively, and the N_2 obviously played a dominant role in the EGR. Therefore, the thermal effect of the EGR on the adiabatic combustion temperature and laminar flame speed of the methane/air was weaker than that of the H_2O and CO_2, but slightly higher than that of introducing N_2 dilution gas. Therefore, the dilution limitation of the EGR on the methane/air was wider than that of the CO_2 and H_2O, but slightly shorter than that of the N_2. In addition, as stated earlier, the chemical effects of the CO_2 and H_2O in the EGR would also affected the flame structure and radicals formation. Consequently, the O, H, OH and CH_3 radicals decreased with importing the 20% EGR in the methane/air mixture as shown in Fig. 8(b).

3.2. Effects of the EGR and hydrogen on the laminar flame speed of the premixed methane/air

Generally, the hydrogen shows the relatively higher laminar burning velocity, diffusivity in air and low heating value, wider lean-burn limitation, smaller flame quenching distance, and lower ignition energy compared to the methane gas [45]. In order to extend the lean-burn limitation and accelerate the combustion rate methane, the hydrogen gas was always added in the methane/air mixture, and formed the premixed methane/hydrogen/air in the paper. Fig. 9 illustrates the effects of the hydrogen enrichment on the laminar flame speed of the methane/air at the stoichiometric air–fuel ratio, initial temperature 298 K and initial pressure 1 bar, and the simulated laminar flame speed of the methane/hydrogen/air was validated against with Halter [46], Hermanns [47], Dirrenberger [48]. Apparently, the laminar flame speed of the methane/hydrogen/air was increased with increasing the hydrogen percentage, which was beneficial to improve significantly the combustion rate, and accelerate the flame propagation. Furthermore, the lean-burn limitation was extended with the increase of the hydrogen ratio in the methane/air, which was conducive to operating at a relatively lower lean condition, and thereby decreasing the adiabatic combustion temperature and reducing the NOx formation. With adding the hydrogen in the methane/air, the hydrogen radical and hydroxyl radicals, which was greatly increased the radical pool such as H, O, OH, HO_2, H_2O_2, and so on. In addition, the reactions of the $OH + H_2 = H + H_2O$, $H + O_2 = O + OH$, $O + H_2 = H + OH$ and $H + HO_2 = 2OH$ were highly sensitivity to the hydrogen addition in the methane/air [49]. Furthermore, the intermediate species could rapidly rise ~ 10 orders of magnitude due to the chemical amplifiers of the H and OH radical, which was easily triggered the branching reactions and chain propagating reactions during the combustion process, and thereby increasing the laminar flame speed of the methane/air.

As stated earlier, although the hydrogen enriched in methane/air will accelerate the combustion rate and improve the combustion efficiency, and even extend the lean-burn limitation, while it will also significantly enhance the combustion temperature, and thereby resulting in high concentration of the NOx formation [50]. In order to

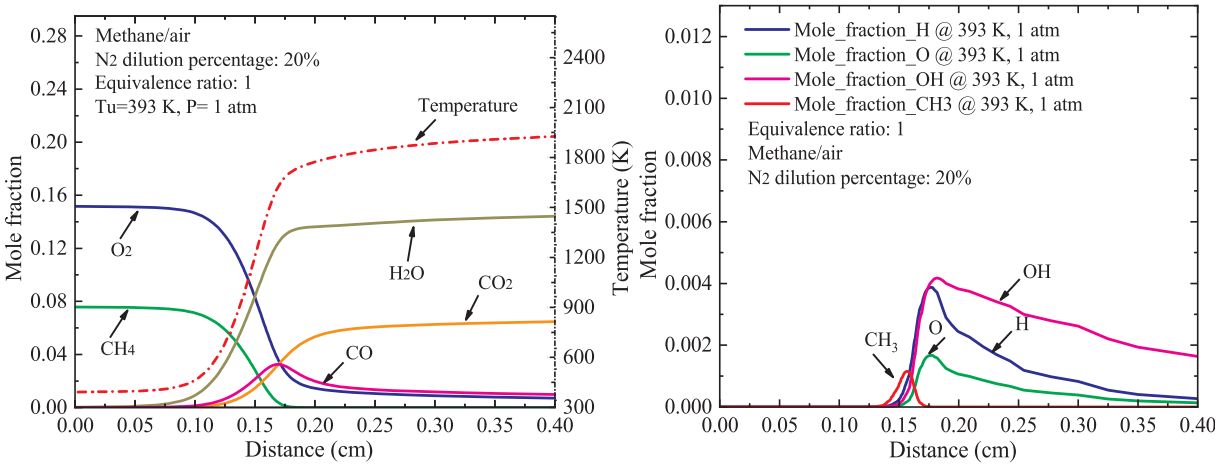

(a) Flame structure profile with N_2 addition (b) Radical reaction rate profiles with N_2 addition

Fig. 7. The flame structure and key radical reaction rate profiles of the methane/air at 393 K and 1 atm with N_2 addition.

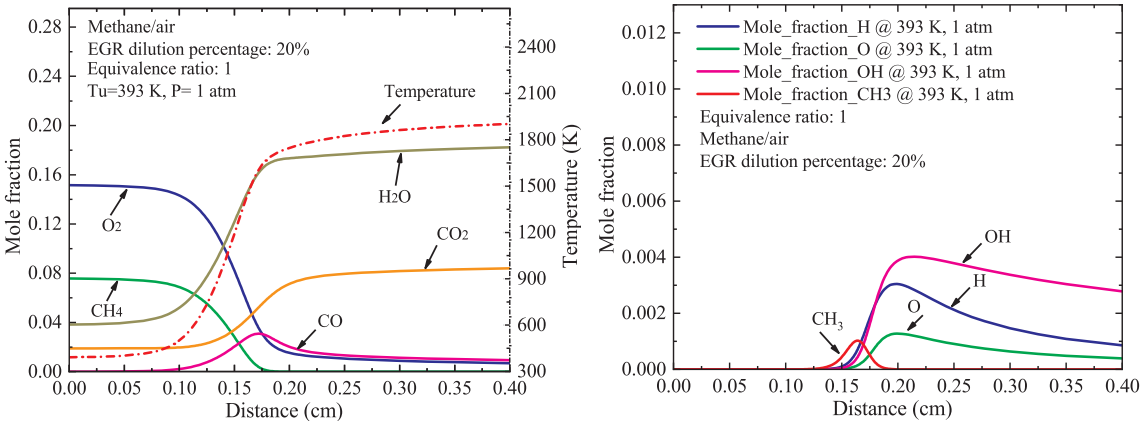

(a) Flame structure profile with EGR addition

(b) Radical reaction rate profiles with EGR addition

Fig. 8. The flame structure and key radical reaction rate profiles of the methane/air at 393 K and 1 atm with EGR addition.

achieve the clean combustion and reduce the NOx formation, the EGR is widely used in most application, such as the internal combustion engine and burner. On the one hand, employing the EGR in the methane/air mixture could decrease the peak combustion temperature, and thereby reducing the NOx formation due to its higher sensitivity to the temperature. On the other hand, with intruding the EGR, the laminar flame speed of the methane/air decrease, and thereby reducing the combustion rate. It is noted that the EGR added into the methane/hydrogen/air mixture in this paper were only considered the CO_2, which was extensively used as an indicator for the EGR ratio during the EGR calibration in the real application, such as the diesel and gasoline engines. Fig. 10 displays the impacts of different EGR ratio on the laminar flame speed of the methane/hydrogen/air at the stoichiometric air–fuel ratio, initial temperature 298 K and initial pressure 1 bar. As illustrates Fig. 10 (a), under the condition of 20% hydrogen enriched in the methane/air, the laminar flame speed of the methane/hydrogen/air was decreased with increasing the EGR ratio, and the inflammability limit of the methane/hydrogen/air was also shrank with increasing the EGR. However, with adding 40% hydrogen enriched in the methane/air, the laminar flame speed of the methane/air was increased, and the inflammability limit of the methane/air was also extended. In addition, under the condition of 40% hydrogen enriched in the methane/air, the laminar flame speed of the methane/hydrogen/air was also decreased with increasing the EGR as illustrated in Fig. 10 (b). But under the condition of 40% hydrogen enriched in the methane/air, the laminar flame speed of the methane/hydrogen/air introduced 10% EGR was almost the same with the pure methane/air, and the lean-burn limitation was almost the same. Therefore, using the hydrogen enriched in the methane/air and coupling with EGR strategy can not only reduce the NOx emissions, but also make up for the lower laminar flame speed caused by EGR.

3.3. *Effects of hydrogen and EGR on the flame structure radical rate profiles of the premixed methane/air*

Fig. 11 and Fig. 12 depict the effects of hydrogen enrichment on the flame structure and radical reaction rate profiles of the methane/air at the stoichiometric air–fuel ratio, initial temperature 298 K and initial pressure 1 bar. Apparently, the flame structure of the methane/hydrogen/air did not change a lot with 20% hydrogen enriched or 40% hydrogen enriched in the methane/air (as illustrated in Fig. 11 (a) and Fig. 12 (a)). However, the radical rate profiles of the methane/hydrogen/air varied greatly, particularly the production and consumption of the H radical. As shown in Fig. 12 (b), under the condition of 40% hydrogen enriched in the methane/air, the mole fraction of the H radical was much higher than that of the 20% hydrogen enriched in the methane/air (as displayed in Fig. 11 (b)). This is attributed to the interactive effects of multiple factors. First, the concentration of the hydrogen in the methane/air was definitely increased, and thereby increasing the H radial through the reactions of the $OH + H_2 = H + H_2O$ and $O + H_2 = H + OH$. Increasing the H and OH radicals were conducive to promoting the chemical reactions due to their high diffusivity [51]. In addition, the laminar flame speed of the methane/hydrogen/air was also increased with increasing the hydrogen ratio, which was

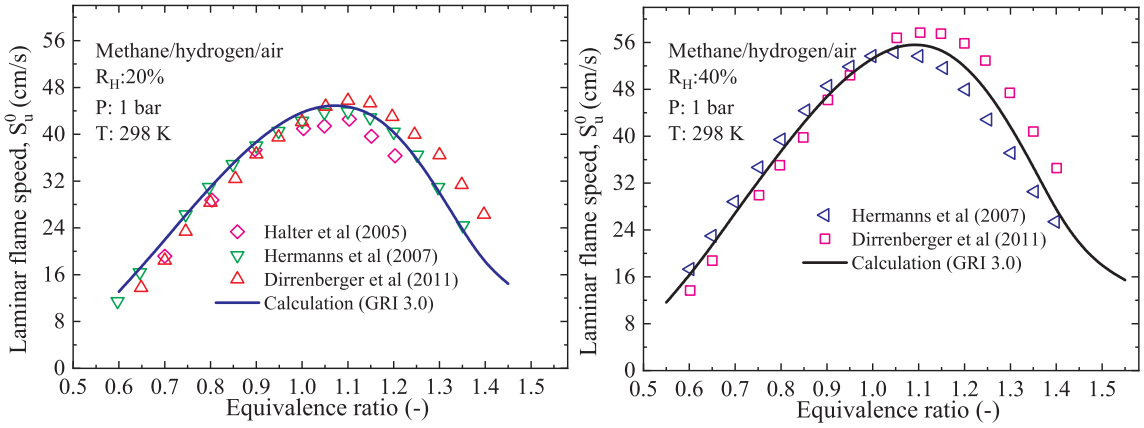

(a) 20% hydrogen on the laminar flame speed of methane/air

(b) 40% hydrogen on the laminar flame speed of methane/air

Fig. 9. Effects of different hydrogen enrichment on methane/air laminar flame speed.

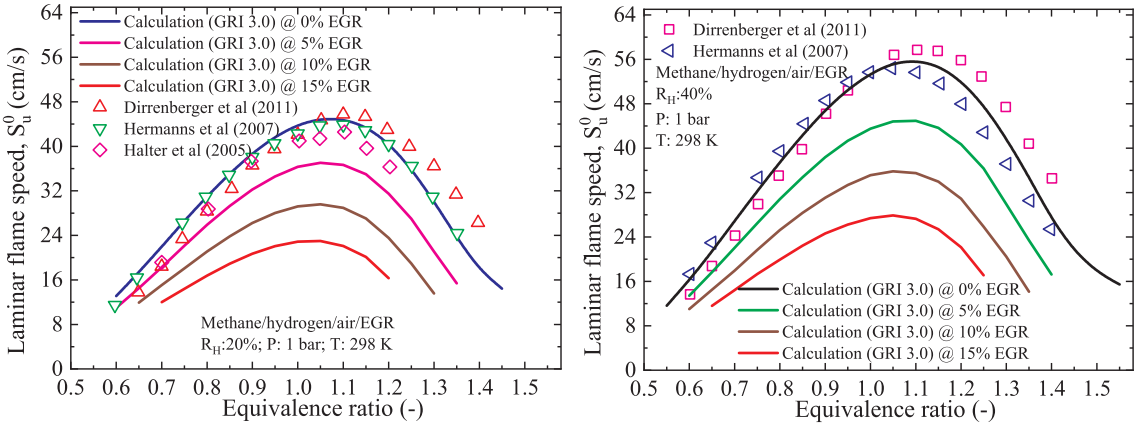

(a) EGR on laminar flame speed of methane/air with 20% hydrogen (b) EGR on laminar flame speed of methane/air with 40% hydrogen

Fig. 10. Effects of EGR on laminar flame speed methane/air with different hydrogen enrichment.

beneficial to accelerate the combustion rate of the methane/hydrogen/air mixture, and ultimately increasing the rate of the heat release during the combustion. Apart from that, the reactions activation energy of the OH + H_2 = H + H_2O and O + H_2 = H + OH were decreased with increasing the hydrogen ratio. Last, the chemical amplifier played increasingly important role in methane/hydrogen/air during the combustion with increasing the hydrogen ratio.

Fig. 13 and Fig. 14 explore the influences of EGR and hydrogen enrichment on the flame structure and radical reaction rate profiles of the methane/air at the stoichiometric air–fuel ratio, initial temperature 298 K and initial pressure 1 bar. With introducing 5% EGR, the thickness of the laminar flame of the methane/hydrogen/air was slightly increased, no matter the ratios of hydrogen enriched in the methane/air (as shown in Fig. 13 (a) and Fig. 14 (a)), and the adiabatic combustion temperature of the methane/hydrogen/air was decreased. On the one hand, the O, H and OH radicals decreased with introducing the EGR in the methane/hydrogen/air mixture due to the chemical effects of the CO_2 and H_2O. On the other hand, the concentration of the methane/hydrogen/air was also decreased, which reduced the radical fraction and the heat release rate, and eventually resulted in decreasing the adiabatic combustion temperature of methane/hydrogen/air. Specifically, at the same level of 5% EGR, the O, H and OH radicals of the methane/hydrogen/air with adding 40% hydrogen were higher than that of the 20% hydrogen addition (as shown in Fig. 14 (b) and Fig. 13 (b)), which was more susceptible to trigger the chain branching reactions of the O + CH_4 = OH + CH_3, H + O_2 = O + OH, H + HO_2 = 2OH, and O + H_2 = H + OH, and the chain propagation reactions of the OH + CH_4 = CH_3 + H_2O and H + CH_4 = CH_3 + H_2. Consequently, the adiabatic combustion temperature of the methane/hydrogen/air with adding 40% hydrogen was higher than that of the 20% hydrogen addition.

Fig. 15 and Fig. 16 reveal the impact of high EGR and hydrogen enrichment on the flame structure and radical reaction rate profiles of the methane/air at the stoichiometric air–fuel ratio, initial temperature 298 K and initial pressure 1 bar. With introducing 15% EGR, the thickness of the laminar flame of the methane/hydrogen/air was significantly increased, no matter the 20% hydrogen or 40% hydrogen enriched in the methane/air (as shown in Fig. 15 (a) and Fig. 16 (a)). Furthermore, the adiabatic combustion temperature of the methane/hydrogen/air was significantly decreased with importing higher EGR ratio. This is largely due to that the chemical and thermal effects of the CO_2 and H_2O in the EGR affected the combustion process of the methane/hydrogen/air. Fortunately, the disadvantages brought from higher EGR ratio were gradually alleviated through adding the hydrogen. Generally, the critical radius and Markstein length of the methane/hydrogen/air were decreased with increasing the hydrogen fraction due to effects of the diffusional-thermal and hydrodynamic instabilities increased [52,53]. In addition, with adding hydrogen in the methane/air, the mole fraction of the O, H and OH radicals were maintained at a relatively higher level during the combustion due to their chain branching reactions and chain propagation reactions (as shown in Fig. 15 (b) and Fig. 16 (b)), which counteracted the side effects introduced by higher EGR, and thereby increasing the laminar flame speed of the methane/hydrogen/air compared to the methane/

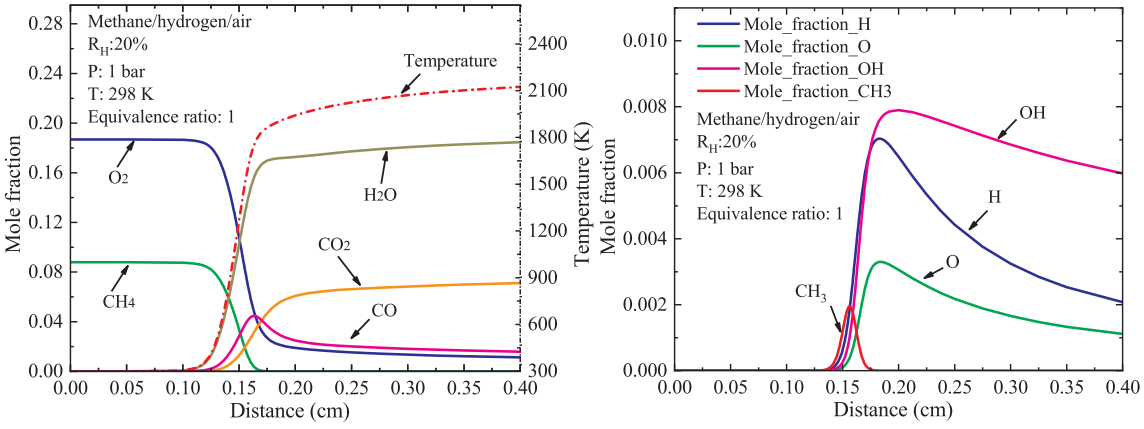

(a) Flame structure profile without EGR addition (b) Radical reaction rate profiles without EGR addition

Fig. 11. The flame structure and key radical reaction rate profiles of hydrogen/methane/air (20% hydrogen) without EGR addition.

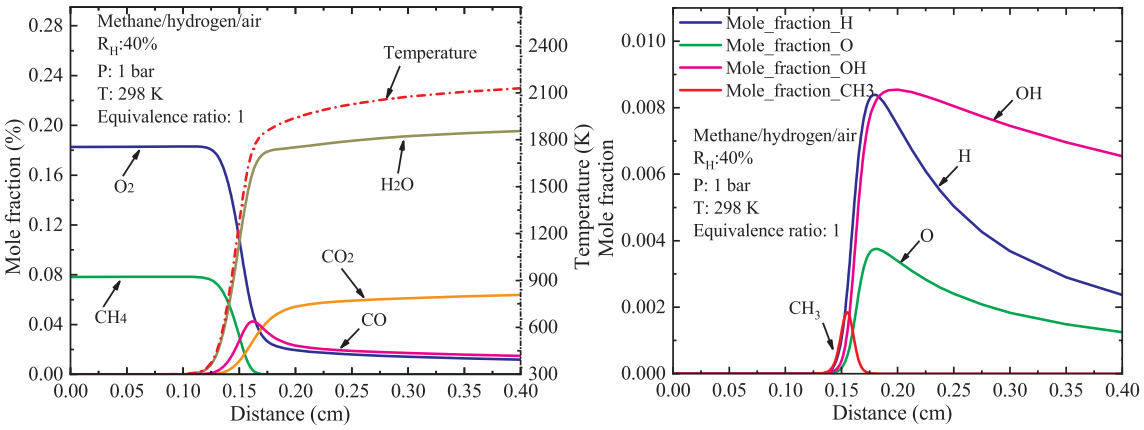

(a) Flame structure profile without EGR addition

(b) Radical reaction rate profiles without EGR addition

Fig. 12. The flame structure and key radical reaction rate profiles of hydrogen/methane/air (40% hydrogen) without EGR addition.

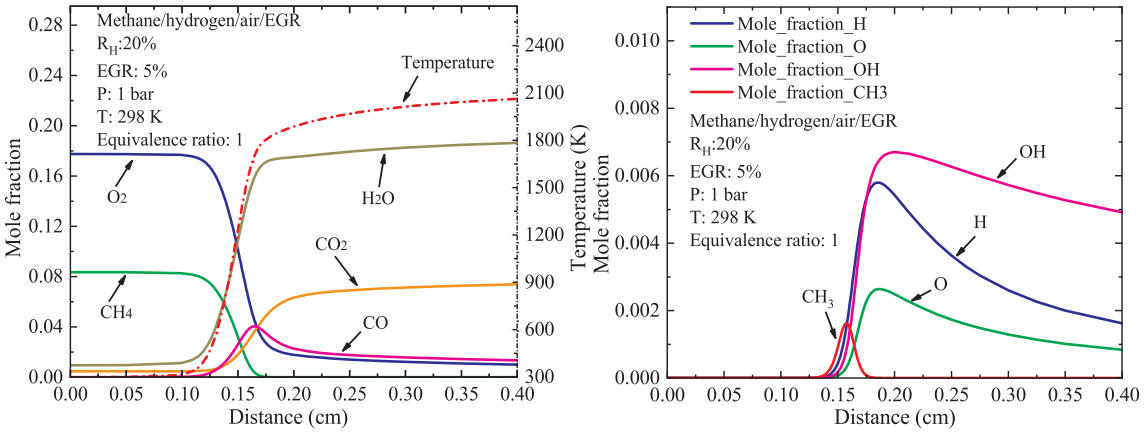

(a) Flame structure profile with 5% EGR addition.

(b) Radical reaction rate profiles with 5% EGR addition.

Fig. 13. The flame structure and key radical reaction rate profiles of hydrogen/methane/air (20% hydrogen) with 5% EGR addition.

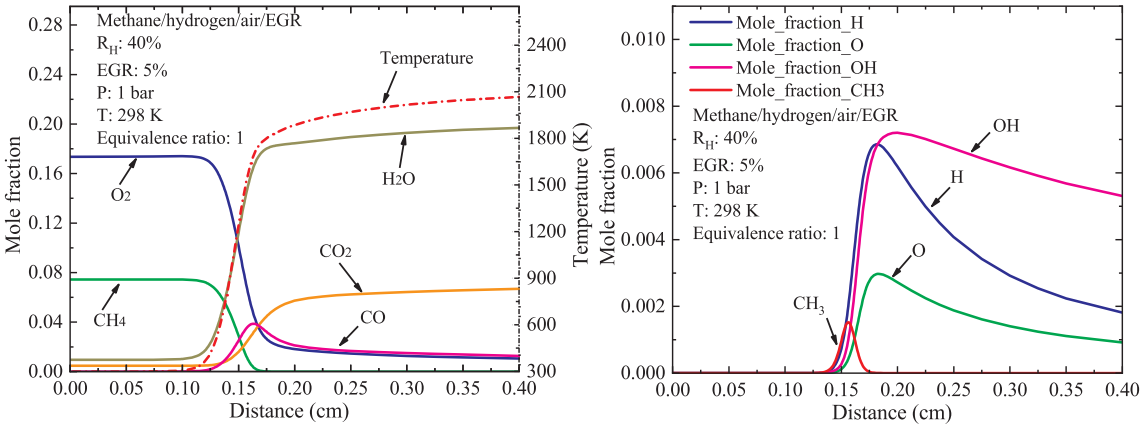

(a) Flame structure profile with 5% EGR addition.

(b) Radical reaction rate profiles with 5% EGR addition.

Fig. 14. The flame structure and key radical reaction rate profiles of hydrogen/methane/air (40% hydrogen) with 5% EGR addition.

air. Strong correlation was also obtained between the laminar flame speed and the radical concentrations of H and OH of the premixed flames in ref. [54,55].

4. Conclusions

In this paper, a numerical investigation on the effects of the dilution gas and hydrogen enrichment on the premixed methane/air was conducted by using the Chemkin package. The chemical effect, thermal effect and dilution effect of the CO_2, H_2O, N_2 and EGR were quantitatively analyzed on the laminar flame speed, laminar flame structure and key radicals profiles of the premixed methane/air mixture under different conditions. Moreover, the artificial species of the FCO_2, FH_2O, FN_2 and FEGR were used in the simulation to separate their chemical and physical effects on the laminar flame speed of the methane/air. Furthermore, the impacts of the hydrogen enrichment coupled with the

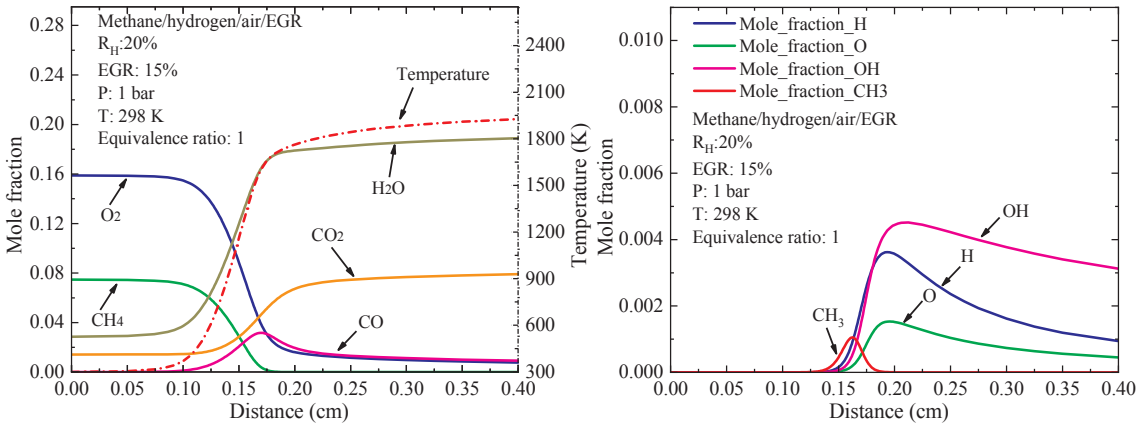

(a) Flame structure profile with 15% EGR addition. (b) Radical reaction rate profiles with 15% EGR addition.

Fig. 15. The flame structure and key radical reaction rate profiles of hydrogen/methane/air (20% hydrogen) with 15% EGR addition.

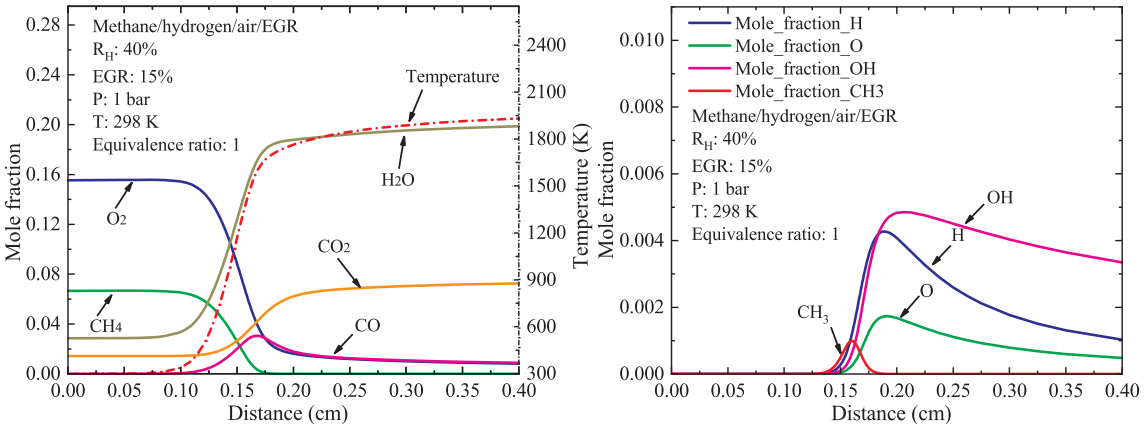

(a) Flame structure profile with 15% EGR addition. (b) Radical reaction rate profiles with 15% EGR addition.

Fig. 16. The flame structure and key radical reaction rate profiles of hydrogen/methane/air (40% hydrogen) with 15% EGR addition.

EGR on the laminar flame speed, laminar flame structure and key radicals profiles of the premixed methane/air mixture was also studied in detail. The main conclusions were summarized as follows:

(1) The chemical effect of the CO_2 dilution gas produced the greatest impacts on the laminar flame speed, adiabatic combustion temperature and key radicals formation of the methane/air, followed by the H_2O vapor, EGR and N_2. In addition, the dilution limitation of the CO_2 in the methane/air was smallest, and followed by the H_2O vapor, EGR and N_2. Moreover, the thermal effect of the CO_2 in the methane/air was strongest due to its highest specific heat capacity, followed by the H_2O vapor, EGR and N_2.

(2) The laminar flame speed and adiabatic combustion temperature of the methane/hydrogen/air was increased with increasing the hydrogen percentage. Furthermore, the lean-burn limitation was extended with the increase of the hydrogen ratio in the methane/air. The radical pool, such as H, O, OH, accelerated the chain branching reactions and the chain propagation reactions, and thereby increasing the effect of the chemical amplifier during the combustion of the premixed L methane/air mixture.

(3) The laminar flame speed of the methane/hydrogen/air was decreased with increasing the EGR ratio, and the inflammability limit of the methane/hydrogen/air was also shrank with increasing the EGR. However, with adding 40% hydrogen enriched in the methane/air, the side effect caused by the EGR on the laminar flame speed of the methane/air could be counteracted, and the inflammability limit of the methane/air was extended. In addition, under the condition of 40% hydrogen enriched in the methane/air, the laminar flame speed of the methane/hydrogen/air introduced 10% EGR was almost the same with the pure methane/air, and the lean-burn limitation was almost the same.

CRediT authorship contribution statement

Xiongbo Duan: Conceptualization, Software, Validation, Investigation, Project administration, Supervision, Writing - original draft. **Yangyang Li:** Writing - review & editing. **Yiqun Liu:** Formal analysis. **Shiheng Zhang:** Formal analysis. **Jinhuan Guan:** Methodology. **Ming-Chia Lai:** Resources. **Jingping Liu:** Funding acquisition.

Declaration of Competing Interest

The authors declare that they have no known competing financial interests or personal relationships that could have appeared to influence the work reported in this paper.

Acknowledgements

This research paper is mainly sponsored by the National Natural Science Foundation of China (NO. 51776061). The authors appreciate the Wayne State University for providing the Chemkin license. In addition, the authors appreciate the anonymous reviewers and the editor for careful reviewing and proving many constructive suggestions to enhance the manuscript.

References

[1] Liu J, Dumitrescu CE. Flame development analysis in a diesel optical engine converted to spark ignition natural gas operation. Appl Energy 2018;230:1205–17.
[2] Li Y, Duan X, Liu Y, Liu J, Guo G, Tang Y. Experimental investigation the impacts of injection strategies coupled with gasoline/ethanol blend on combustion, performance and emissions characteristics of a GDI spark-ignition engine. Fuel 2019;256:115910.
[3] Duan X, Liu J, Yao J, Chen Z, Wu C, Chen C, et al. Performance, combustion and knock assessment of a high compression ratio and lean-burn heavy-duty spark-ignition engine fuelled with n-butane and liquefied methane gas blend. Energy. 2018;158:256–68.
[4] Khan AR, Ravi MR, Ray A. Experimental and chemical kinetic studies of the effect of H2 enrichment on the laminar burning velocity and flame stability of various multicomponent natural gas blends. Int J Hydrogen Energy 2019;44:1192–212.
[5] Li G, Zhou M, Zhang Z, Liang J, Ding H. Experimental and kinetic studies of the effect of CO2 dilution on laminar premixed n-heptane/air flames. Fuel 2018;227:355–66.
[6] Duan X, Liu Y, Liu J, Lai M-C, Jansons M, Guo G, et al. Experimental and numerical investigation of the effects of low-pressure, high-pressure and internal EGR configurations on the performance, combustion and emission characteristics in a hydrogen-enriched heavy-duty lean-burn natural gas SI engine. Energy Convers Manage 2019;195:1319–33.
[7] Hermanns RTE, Konnov AA, Bastiaans RJM, de Goey LPH, Lucka K, Köhne H. Effects of temperature and composition on the laminar burning velocity of CH4 + H2 + O2 + N2 flames. Fuel 2010;89:114–21.
[8] Huang Z, Zhang Y, Zeng K, Liu B, Wang Q, Jiang D. Measurements of laminar burning velocities for natural gas–hydrogen–air mixtures. Combust Flame 2006;146:302–11.
[9] Hu E, Huang Z, He J, Miao H. Experimental and numerical study on lean premixed methane–hydrogen–air flames at elevated pressures and temperatures. Int J Hydrogen Energy 2009;34:6951–60.
[10] Chen Y, Wolk B, Mehl M, Cheng WK, Chen J-Y, Dibble RW. Development of a reduced chemical mechanism targeted for a 5-component gasoline surrogate: A case study on the heat release nature in a GCI engine. Combust Flame 2017;178:268–76.
[11] Chen Z, Tang C, Fu J, Jiang X, Li Q, Wei L, et al. Experimental and numerical investigation on diluted DME flames: Thermal and chemical kinetic effects on laminar flame speeds. Fuel 2012;102:567–73.
[12] Mazas AN, Fiorina B, Lacoste DA, Schuller T. Effects of water vapor addition on the laminar burning velocity of oxygen-enriched methane flames. Combust Flame 2011;158:2428–40.
[13] Chen Z. On the accuracy of laminar flame speeds measured from outwardly propagating spherical flames: Methane/air at normal temperature and pressure. Combust Flame 2015;162:2442–53.
[14] Liu C, Song H, Zhang P, Wang Z, Wooldridge MS, He X, et al. A rapid compression machine study of autoignition, spark-ignition and flame propagation characteristics of H2/CH4/CO/air mixtures. Combust Flame 2018;188:150–61.
[15] Liu J, Dumitrescu CE. Methodology to separate the two burn stages of natural-gas lean premixed-combustion inside a diesel geometry. Energy Convers Manage 2019;195:21–31.
[16] Konnov AA, Mohammad A, Kishore VR, Kim NI, Prathap C, Kumar S. A comprehensive review of measurements and data analysis of laminar burning velocities for various fuel + air mixtures. Prog Energy Combust Sci 2018;68:197–267.
[17] Law CK, Sung CJ, Wang H, Lu T. Development of comprehensive detailed and reduced reaction mechanisms for combustion modeling. AIAA journal. 2003;41:1629–46.
[18] De Goey L, Van Oijen J, Kornilov V, ten Thije BJ. Propagation, dynamics and control of laminar premixed flames. Proc Combust Inst 2011;33:863–86.
[19] Bunsen R. Ueber die Temperatur der Flammen des Kohlenoxyds und Wasserstoffs. Ann Phys 1867;207:161–79.
[20] Konnov AA, Riemeijer R, Kornilov V, de Goey L. 2D effects in laminar premixed flames stabilized on a flat flame burner. Exp Therm Fluid Sci 2013;47:213–23.
[21] Simmons R, Wolfhard H. Some limiting oxygen concentrations for diffusion flames in air diluted with nitrogen. Combust Flame 1957;1:155–61.
[22] Yu H, Han W, Santner J, Gou X, Sohn CH, Ju Y, et al. Radiation-induced uncertainty in laminar flame speed measured from propagating spherical flames. Combust Flame 2014;161:2815–24.
[23] Egolfopoulos FN, Hansen N, Ju Y, Kohse-Höinghaus K, Law CK, Qi F. Advances and challenges in laminar flame experiments and implications for combustion chemistry. Prog Energy Combust Sci 2014;43:36–67.
[24] Faghih M, Han W, Chen Z. Effects of Soret diffusion on premixed flame propagation under engine-relevant conditions. Combust Flame 2018;194:175–9.
[25] Chica Cano JP, Cabot G, Foucher F, de Persis S. Effects of oxygen enrichment and water dilution on laminar methane flames at high pressure. Fuel 2018;225:499–508.
[26] Hu E, Huang Z, Liu B, Zheng J, Gu X. Experimental study on combustion characteristics of a spark-ignition engine fueled with natural gas–hydrogen blends combining with EGR. Int J Hydrogen Energy 2009;34:1035–44.
[27] Mitu M, Giurcan V, Razus D, Oancea D. Inert gas influence on the laminar burning velocity of methane-air mixtures. J Hazard Mater 2017;321:440–8.
[28] Xiang L, Chu H, Ren F, Gu M. Numerical analysis of the effect of CO2 on combustion characteristics of laminar premixed methane/air flames. J Energy Inst 2019;92:1487–501.
[29] Fells I, Rutherford A. Burning velocity of methane-air flames. Combust Flame 1969;13:130–8.
[30] Khan AR, Anbusaravanan S, Kalathi L, Velamati R, Prathap C. Investigation of dilution effect with N2/CO2 on laminar burning velocity of premixed methane/oxygen mixtures using freely expanding spherical flames. Fuel 2017;196:225–32.
[31] Albin E, Nawroth H, Göke S, d'Angelo Y, Paschereit CO. Experimental investigation of burning velocities of ultra-wet methane–air–steam mixtures. Fuel Process Technol 2013;107:27–35.
[32] Xie Y, Wang J, Xu N, Yu S, Huang Z. Comparative study on the effect of CO2 and H2O dilution on laminar burning characteristics of CO/H2/air mixtures. International Journal of Hydrogen Energy. 2014;39:3450-8.
[33] Liu J, Zhang X, Wang T, Hou X, Zhang J, Zheng S. Numerical study of the chemical, thermal and diffusion effects of H 2 and CO addition on the laminar flame speeds of methane–air mixture. Int J Hydrogen Energy 2015;40:8475–83.
[34] Schefer RW, Wicksall D, Agrawal A. Combustion of hydrogen-enriched methane in a lean premixed swirl-stabilized burner. Proc Combust Inst 2002;29:843–51.
[35] Ilbas M, Crayford A, Yilmaz I, Bowen P, Syred N. Laminar-burning velocities of hydrogen–air and hydrogen–methane–air mixtures: An experimental study. Int J Hydrogen Energy 2006;31:1768–79.
[36] Zuo Z, Pei Y, Qin J, Xu H, Lu L. Laminar burning characteristics of premixed methane-dissociated methanol-air mixtures under lean burn conditions. Appl Therm Eng 2018;140:304–12.
[37] Turns SR. Introduction to combustion: McGraw-Hill Companies; 1996.
[38] Gaydon AG, Flames WHG. their structure, radiation, and temperature. Halsted Press; 1979.
[39] Smith GP, Golden DM, Frenklach M, Moriarty NW, Eiteneer B, Goldenberg M, et al. GRI 3.0 Mechanism. Gas Research Institute (http://www me berkeley edu/gri_mech). 1999.
[40] Kee RJ, Grcar JF, Smooke MD, Miller JA, Meeks E. PREMIX: a Fortran program for modeling steady laminar one-dimensional premixed flames. Sandia National Laboratories Report. 1985.
[41] Hu E, Jiang X, Huang Z, Iida N. Numerical study on the effects of diluents on the laminar burning velocity of methane–air mixtures. Energy Fuels 2012;26:4242–52.
[42] Galmiche B, Halter F, Foucher F, Dagaut P. Effects of Dilution on Laminar Burning Velocity of Premixed Methane/Air Flames. Energy Fuels 2011;25:948–54.
[43] Xie Y, Wang J, Zhang M, Gong J, Jin W, Huang Z. Experimental and Numerical Study on Laminar Flame Characteristics of Methane Oxy-fuel Mixtures Highly Diluted with CO2. Energy Fuels 2013;27:6231–7.
[44] Le Cong T, Dagaut P. Effect of water vapor on the kinetics of combustion of hydrogen and natural gas: experimental and detailed modeling study. ASME Turbo Expo 2008: Power for Land, Sea, and Air: American Society of Mechanical Engineers Digital Collection; 2008. p. 319-28.
[45] Duan X, Li Y, Liu J, Guo G, Fu J, Zhang Q, et al. Experimental study the effects of various compression ratios and spark timing on performance and emission of a lean-burn heavy-duty spark ignition engine fueled with methane gas and hydrogen blends. Energy. 2019;169:558–71.
[46] Halter F, Chauveau C, Djebaïli-Chaumeix N, Gökalp I. Characterization of the effects of pressure and hydrogen concentration on laminar burning velocities of methane–hydrogen–air mixtures. Proc Combust Inst 2005;30:201–8.
[47] Hermanns RTE, Kortendijk J, Bastiaans R, De Goey L. Laminar burning velocities of methane-hydrogen-air mixtures. Praca doktorska, Technische Universitat Eindhoven. 2007.
[48] Dirrenberger P, Le Gall H, Bounaceur R, Herbinet O, Glaude P-A, Konnov A, et al. Measurements of laminar flame velocity for components of natural gas. Energy Fuels 2011;25:3875–84.
[49] Wang J, Huang Z, Tang C, Miao H, Wang X. Numerical study of the effect of hydrogen addition on methane–air mixtures combustion. Int J Hydrogen Energy 2009;34:1084–96.
[50] Liu J, Duan X, Yuan Z, Liu Q, Tang Q. Experimental study on the performance, combustion and emission characteristics of a high compression ratio heavy-duty spark-ignition engine fuelled with liquefied methane gas and hydrogen blend. Appl Therm Eng 2017;124:585–94.
[51] Echeverri-Uribe C, Amell AA, Rubio-Gaviria LM, Colorado A, McDonell V. Numerical and experimental analysis of the effect of adding water electrolysis products on the laminar burning velocity and stability of lean premixed methane/air flames at sub-atmospheric pressures. Fuel 2016;180:565–73.
[52] Hu E, Huang Z, He J, Zheng J, Miao H. Measurements of laminar burning velocities and onset of cellular instabilities of methane–hydrogen–air flames at elevated pressures and temperatures. Int J Hydrogen Energy 2009;34:5574–84.
[53] Tang C, Huang Z, Law C. Determination, correlation, and mechanistic interpretation of effects of hydrogen addition on laminar flame speeds of hydrocarbon–air mixtures. Proc Combust Inst 2011;33:921–8.
[54] Hu E, Huang Z, He J, Jin C, Zheng J. Experimental and numerical study on laminar burning characteristics of premixed methane–hydrogen–air flames. Int J Hydrogen Energy 2009;34:4876–88.
[55] Cheng Y, Tang C, Huang Z. Kinetic analysis of H2 addition effect on the laminar flame parameters of the C1–C4 n-alkane-air mixtures: From one step overall assumption to detailed reaction mechanism. Int J Hydrogen Energy 2015;40:703–18.